

# Online Energy Consumption Monitoring of Wireless Testbed Infrastructure through the NITOS EMF Framework

Stratos Keranidis<sup>⊕</sup>, Giannis Kazdaridis<sup>⊕</sup>, Virgilios Passas<sup>⊕</sup>,  
Thanasis Korakis<sup>⊕</sup>, Iordanis Koutsopoulos\* and Leandros Tassioulas<sup>⊕</sup>  
<sup>⊕</sup>Department of Computer and Communication Engineering, University of Thessaly, Greece  
<sup>⊖</sup>Centre for Research and Technology Hellas, CERTH, Greece  
<sup>\*</sup>Department of Computer Science Athens University of Economics and Business, Greece  
{efkerani, iokazdarid, vipassas, korakis, leandros}@uth.gr, jordan@aueb.gr

## ABSTRACT

Development of energy-efficient protocols and algorithms requires in-depth understanding of the power consumption characteristics of real world devices. To this aim, energy efficiency analysis is performed by the research community, mainly focusing on the development of power consumption models. However, recent studies [1] have highlighted the inability of existing models to accurately estimate energy consumption even in non-composite scenarios, where the operation of a single device is analyzed. The inability of such models is further highlighted under real life scenarios, where the impact induced by the simultaneous operation of several devices renders the application of traditional models completely inappropriate. As a result, energy efficiency evaluation under complex configurations and topologies, needs to be experimentally investigated through the application of online monitoring solutions. In this work, we propose the innovative NITOS Energy consumption Monitoring Framework (EMF) able to support online monitoring of energy expenditure, along with the experiment execution. The developed framework is built on a distributed network of low-cost, but highly accurate devices and is fully integrated with the large-scale wireless NITOS testbed. Framework evaluation is performed under both low-level experiments that demonstrate the platform's high-level accuracy, as well as through high-level experiments that showcase how online and distributed monitoring can facilitate energy performance assessment of realistic testbed experiments.

## Categories and Subject Descriptors

C.2.1 [Computer-Communication Networks]: Network Architecture and Design - Wireless Communications

## Keywords

Energy, Power, Monitoring, 802.11a/g/n, Experimentation

Permission to make digital or hard copies of all or part of this work for personal or classroom use is granted without fee provided that copies are not made or distributed for profit or commercial advantage and that copies bear this notice and the full citation on the first page. Copyrights for components of this work owned by others than ACM must be honored. Abstracting with credit is permitted. To copy otherwise, or republish, to post on servers or to redistribute to lists, requires prior specific permission and/or a fee. Request permissions from [permissions@acm.org](mailto:permissions@acm.org).  
*WiNTECH'13*, September 30 2013, Miami, Florida, USA  
Copyright 2013 ACM 978-1-4503-2364-2/13/09 ...\$15.00.  
<http://dx.doi.org/10.1145/2505469.2505478>.

## 1. INTRODUCTION

The unprecedented penetration of "smart" mobile devices in everyday use cases, has greatly affected the trends followed by vendors developing such equipment. First, the need for offering ubiquitous network coverage, has led the industry in equipping these devices with several wireless interfaces (WiFi, Bluetooth, 3G, LTE, WiMAX), to facilitate parallel network access. Second, in an effort to meet the increasing requirements generated by the use of resource-demanding applications, high-end mobile devices feature multi-core processors, high-resolution displays and support increased data rate communication technologies. Especially in the case of smartphone platforms, the energy greedy profile of the supported state-of-the-art wireless technologies may induce up to 50% of the total platform power consumption [2], under typical use case scenarios. The increased energy demands of such technologies cannot be successfully met, due to the limited energy capacity [3] that existing battery technologies are able to offer.

The overall goal, towards alleviating this unique performance discrepancy, is to reduce energy consumption wherever possible. To this aim, several recent research studies [4, 5, 6, 7] in the field of wireless networking have focused on reducing the total amount of energy consumed during the wireless medium access and communication operations. In this context, accurate energy consumption assessment needs to be applied by the research community, as a means of evaluating the energy efficiency of the proposed protocols and architectures. Researchers working on wireless sensor networks can base their evaluations on detailed low level specifications [8, 9] provided by developers of widely adopted sensor platforms (Tmote Sky, MICAz). However, this is not the case with vendors that develop wireless transceivers for everyday use devices, such as laptops, smartphones or tablets, where only limited information on nominal consumption is publicly provided [10]. Even in cases that accurate data sheet specifications are available, power consumption models that are based on such accurate measurements, fail to successfully calculate energy expenditure under complex configurations and topologies.

In order to enable experimenters to accurately evaluate the energy efficiency of the proposed protocols, under real world scale and settings, advanced methodologies and solutions need to be developed. In this work, we propose the innovative NITOS EMF framework that is fully integrated

with the large-scale wireless NITOS testbed [11] and provides for online gathering of energy measurements, through a distributed network of low-cost, but highly accurate devices.

## 1.1 Related Work

As previously stated, a great variety of research efforts has proposed energy-efficient protocols and architectures, towards moving to "greener" solutions in telecommunications. Mechanisms proposed in recent works range from scheduling of sleep intervals and antenna configurations [12], to reduction of time spent during idle listening periods [4] and application of adaptive transmit power and physical layer (PHY) rate control [5]. The approaches above, jointly follow the methodology of first identifying key functions that exacerbate energy expenditure and subsequently attempt to control the induced impact by efficiently scheduling their operation. Other relevant works focus more on energy consumption characterisation of specific technologies, such as the power-hungry IEEE802.11n [13], or specific platforms, such as the energy-limited smartphones [6, 7]. Trying to address the limited level of detail provided by the industry, several works [14, 2] present extensive measurements that assess the impact of low-level configurations on the overall power consumption of various platforms. In order to gather such detailed measurements, either commercial sensing hardware or custom measurement setups are employed, which result in varying levels of obtained accuracy and reliability.

In an effort to support evaluation under definite measurement setups, a limited variety of approaches have developed proper energy consumption monitoring frameworks for testbeds that specifically target wireless sensor networks [15] or data centers [16]. Similarly, the work in [17] proposes a framework developed for energy consumption monitoring of real WLAN deployments. However, this framework is restricted in characterising the consumption at the level of complete device (router). The importance of monitoring consumption of both the wireless network interface card (NIC) and the complete device as a total, in deriving hitherto unexploited tradeoffs, is highlighted in [1]. Based on comparison of energy consumed at the transceiver and the complete device level, this work proposes a novel energy model that contrasts traditional approaches, which neglect the fraction of energy consumed while each frame crosses the protocol stack.

This paper is organized as follows. In sections 2,3 and 4, we present the required platform specifications, the followed measurement methodology and detail the various framework components accordingly. In section 5, we present extensive experiments that evaluate the platform's capabilities, while in section 6 we point out conclusions and directions for future work.

## 2. PLATFORM SPECIFICATIONS

The overall goal of the proposed work is to turn the rather challenging task of online energy consumption monitoring into an automated procedure that is available to wireless testbed experimenters. Below, we list the various characteristics that the platform should feature, along with the implementation choices that we followed:

- **Non-intrusive operation:** The normal network operation should not be affected by the monitoring procedure, in order not to result in imprecise results. Our

solution runs on external hardware, which does not interfere with the measured devices.

- **Online monitoring:** Online monitoring needs to be applied, towards energy efficiency evaluation under complex configurations and topologies. The proposed framework allows for online gathering of measurements in parallel with execution of long-term experiments.
- **Distributed architecture:** Assessment of the impact induced by simultaneous operation of collocated network components, requires the development and application of distributed energy consumption monitoring solutions. The proposed framework is composed of distributed communication enabled components.
- **High sampling rate:** State-of-the-art wireless technologies are capable of high transmission rates, which generates the necessity for energy monitoring devices to feature high sampling rate components that allow monitoring of short duration events (in the order of  $\mu s$ ). The developed platform achieves twice the minimum required sampling rate.
- **High sampling accuracy:** Wireless testbed infrastructure may operate in states that result in similar energy consumption, thus necessitating the application of high accuracy sampling equipment able to distinguish between the energy consumption induced in such operational states. The custom developed hardware achieves accuracy in the order of milliwatts.
- **Adaptive to heterogeneous infrastructure:** Due to the existence of several heterogeneous types of interfaces, protocols and architectures, connectivity of the developed solutions with the components under test should be easily setup in all cases. The followed measurement procedure is rather generic and allows for power consumption monitoring of any device type.
- **Low-cost hardware:** The extended scale and increasing scalability of modern experimental infrastructure require that the developed hardware components are of low cost to allow for the distributed deployment of several monitoring devices. The developed hardware solution introduces a total cost of less than €80.

## 3. MEASUREMENT METHODOLOGY

In order to estimate the instantaneous power consumption of any device, we follow a widely adopted power measurement procedure, which requires the placement of a high precision, low impedance current-shunt resistor ( $R$ ) of a known resistance value, in series with the power source and the power supply pin of the device to be measured. The exact measurement setup described above is presented in Fig. 1.

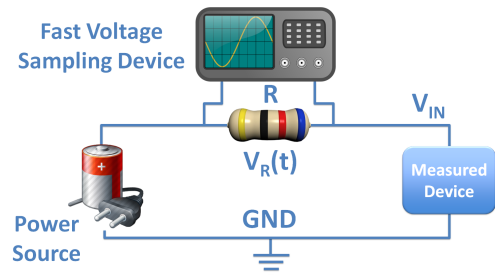


Figure 1: Representation of Power Measurement setup

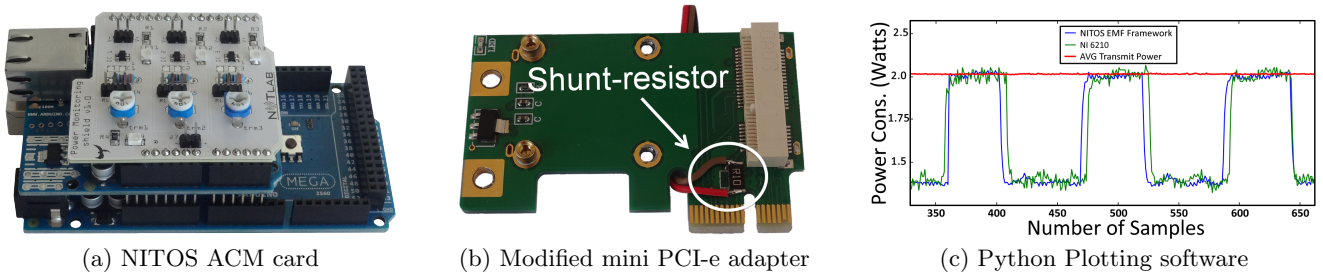


Figure 2: NITOS ACM card and accompanying hardware and software components

By consistently measuring the voltage ( $V_R(t)$ ) across the current-shunt resistor through proper voltage metering equipment, we are able to extract the instantaneous current draw of the device, based on Ohm’s law. The instantaneous power consumption can be calculated as the product of the input voltage  $V_{IN}$  and the measured current draw:

$$P(t) = V_{IN} \frac{V_R(t)}{R} \quad (1)$$

In order to estimate the total energy consumption during specific events, we first need to estimate the event’s duration. Total energy consumed over an interval ( $t_0 \dots t_1$ ) is the integral of power consumption over the specified time duration ( $Dt = t_1 - t_0$ ), calculated as:

$$E(Dt) = \frac{V_{IN}}{R} \int_{t_0}^{t_1} V_R(t) dt \quad (2)$$

For instance, the duration of a single frame transmission or reception can be directly obtained as the product of the frame length and the configured PHY-layer bit rate. Subsequently, energy consumption can be obtained as the integral of the power consumption over the calculated duration.

## 4. NITOS EMF FRAMEWORK

NITOS EMF, which integrates both hardware and software components, manages to implement the aforementioned power measurement approach. Below, we detail the platform characteristics and describe how the framework has been integrated with the testbed architecture.

### 4.1 Hardware Components

The developed hardware device, is built on top of the first version of the NITOS Chassis Manager (CM) Card [18], which was initially used to control the operational status of testbed nodes. The advanced version of the card (*NITOS ACM*), which is presented in Fig. 2(a), is mainly composed of Arduino compatible open-source components, but also features custom developed hardware. The various hardware components are detailed below:

#### Arduino Mega 2560

The developed card is based on the low cost Arduino Mega 2560 board, featuring the ATmega2560 [19] 8-bit microcontroller that runs at 16MHz and operates at 5 Volts. The ATmega2560 integrates a 16 channel Analog to Digital Converter (ADC), with a resolution of 10-bit (i.e. 1024 different values), to provide for sampling of analog signals. We use the integrated ADC to sample the voltage across the shunt resistor as presented in Fig. 1. We decided to use the Arduino Mega 2560, as it offers 256 KB of flash memory and 8 KB of SRAM, which features are required for the efficient operation of the developed software components.

#### Ethernet Shield with SD card

In order to provide for distributed measurements, the card should feature network communication capabilities. To this aim, we decided to equip the card with the Arduino Ethernet Shield, which features the embedded Wiznet W5100 network controller that implements a network (IP) stack capable of both TCP and UDP communication. Another key characteristic of this shield, is the embedded micro SD slot that provides the board with external storage capabilities, enabling for long-term logging of sampled data.

#### Custom Shield integrated with the INA139 IC

Since the integrated ADC is not able to accurately digitize the attained voltage levels on shunt resistors in cases where the monitored voltage drop is minimally varied (mV range), we equipped the developed card with the Texas Instruments INA139 [20] Integrated Circuit. INA139 is a high-side current-shunt monitor that converts a differential input voltage to an amplified value, where the amplification level is controlled through an external load resistor ( $R_L$ ) and can be set from 1 to over 100. The amplification accuracy of the INA139 IC is directly dependent on the selection of the current-shunt ( $R$ ) and load resistor ( $R_L$ ) values.

In order to decide about the proper value of the shunt resistor, we have to consider the average consumption of the device that will be measured. Considering that commercial wireless NICs have an average consumption of 2 Watts we select to use a shunt resistor of  $0.1 \Omega$ , which attains 60 mV of shunt voltage that is within the specified limits [20]. Considering the configuration of the  $R_L$  resistor, we decided to use a  $30 \text{ K}\Omega$  resistor, which meets the maximum output voltage requirement of 2.725 Volts that is specified in the INA139 data sheet. Having properly configured the resistor values that control the INA139, we then designed and fabricated a Printed Circuit Board (PCB), which can be directly integrated on the Arduino board. The designed PCB, which can be seen on top of the Arduino hardware in Fig. 2(a), features three individual INA139 and all the required electrical components, providing for power consumption monitoring of multiple devices.

#### Custom mini-PCIE adapter

Having decided about the proper value of the current-shunt resistor, we next had to attach it in series with the power supply pins of several wireless NICs. In order to ease the interception of the power supply pins and refrain from modifying each different type of NIC, we followed a more applicable approach and inserted the current-shunt resistors on communication bus adapter cards. Fig. 2(b) illustrates a modified pci-e to mini pci-e adapter card that is attached with a high-precision current-shunt resistor of  $0.1 \Omega$ .

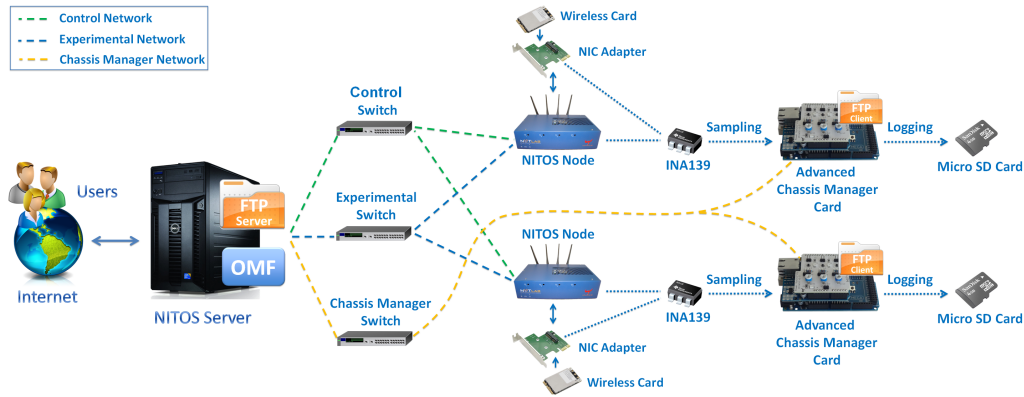


Figure 3: Integration of NITOS EMF framework with the overall testbed architecture

## 4.2 Software Components

Towards rendering the described hardware platform into a functional framework, we developed appropriate software to control the ACM cards and integrate them with the testbed.

### Arduino Software

The sampling rate of approximately 9 KHz that is supported by the default Arduino configurations, is not sufficient for sampling events that last for time intervals in the order of  $\mu$ s. We consider transmissions of typical MPDU frames of 1534 bytes length as the shortest in duration event, which requires approximately  $27\mu$ s to be transmitted at the  $TX_R$  of 450 Mbps. As a result, we need to achieve sampling rate higher than 37KHz, in order to be able to monitor such transmissions.

To overcome this issue, we modified the default ATmega2560 ADC configurations that control the achievable sampling rate. First of all, we configured the ADC to operate in the free-running mode, which enables the ADC to continuously perform conversions without requiring proper signalling from the  $\mu$ C. Through this modification, we enable SD card logging of sampled data to take place in parallel with ADC conversions, efficiently increasing the amount of time spent in sample acquisition. Moreover, we properly modified the clock speed of the ADC prescaler from the default value of 125KHz to 1MHz, following the approaches in [21, 22]. Finally, we efficiently exploited the available SRAM of ATmega2560 to directly store up to 13 blocks of 512 bytes buffers into the SD card. Based on the aforementioned modifications we manage to achieve the remarkably increased sampling rate of 63 KHz, with 10-bit resolution, while only reducing the perceived accuracy by approximately 11% [23]. Additionally, we modified the default ADC voltage reference to 2.5 Volts to enable conversions of higher accuracy. The developed platform has been evaluated in comparison with the high-end NI-6210 data acquisition (DAQ) module [24] and proved of providing measurements of similar accuracy in the range under consideration.

Towards providing for remote control of the distributed cards, we developed a tiny Web Server that is based on the Arduino Ethernet Library and operates on each individual ACM card. Through the transmission of custom UDP packets, we can remotely trigger the measurement acquisition procedure. Furthermore, we developed an FTP service that provides for collection of captured data in a distributed way.

### Python Software

We also developed a set of Python scripts that enable direct

access to the collected results and moreover precise power and energy consumption calculations. Fig. 2(c) presents the implemented plotting component and also depicts a comparison between measurements gathered through the developed framework and the high-end NI-6210 device. The overall set of developed software components is publicly available for users of the NITOS testbed.

### Integration with OMF

To enable ease of use of the developed framework, we integrated its functionalities into the OMF cControl and Management Framework [25]. Based on this integration, experimenters can fully configure the operation of the ACM cards and moreover collect and access the gathered measurements through the OMF Measurement Library [26].

## 4.3 Framework Architecture

The proposed framework has been directly integrated with the underlying network architecture of the NITOS testbed.

### 4.3.1 NITOS Testbed

NITOS testbed currently offers 50 wireless nodes and provides open remote access to any researchers who would like to test their protocols in a real-life wireless network. The testbed architecture is illustrated in the left part of Fig. 3. Two Gigabit Ethernet switches interconnect the nodes with NITOS server, namely the *Control* switch that provide for control of experiment execution and measurement collection and the *Experimental* switch, which can be used for conducting wired experiments. A third Gigabit Ethernet, namely the *Chassis Manager* switch, is dedicated in controlling the operational status of the nodes through the transmission of custom http requests that control solid state relays on the Chassis Manager cards. NITOS nodes feature up to 3 wireless NICs, using the Atheros AR5424 and AR9380 chipsets.

### 4.3.2 Integration of NITOS EMF with the Testbed

Currently 20 of the nodes are attached with ACM cards, which together with the modified mini-PCIe adapters and node power supplies, enable for online energy consumption monitoring in a distributed way. The integration of the NITOS EMF framework with the overall testbed architecture is illustrated in Fig. 3. NITOS ACM cards are properly configured to monitor both the consumption of the NIC in an individual way, as well as the total consumption of each node. Through the *Chassis Manager* switch and the developed FTP service, measurements logged locally in the Micro SD card of each individual ACM card are transferred in a distributed way to the NITOS server.

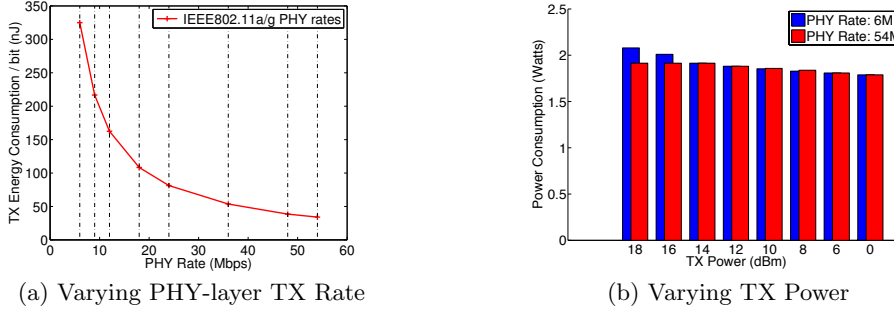


Figure 4: Consumption of AR5424 NIC during frame transmission across different configurations

## 5. EXPERIMENTAL EVALUATION

Based upon NITOS testbed that implements the proposed framework, numerous experiments were conducted, and the results obtained are analyzed in this section. The first set of experiments has been designed to demonstrate the ability of the framework to accurately monitor the effect induced by low-level configurations in the overall consumption of wireless NICs. As the range of the available low-level configurations that can highly impact energy consumption is rather extended, we detail our experimental results and findings in a technical report [27] and only present a representative sample of the obtained results in this work.

Through the second set of experiments, we aim at showcasing how the online and distributed sensing capabilities of the proposed framework can aid towards realistic evaluation of wireless protocols in terms of energy efficiency. In this context, we conduct two experiments that implement an everyday life scenario of simultaneous file uploading by multiple peers, under varying configurations and channel conditions. In parallel with the experiment execution, we monitor the power consumption of each node’s NIC and thus we manage to get a high level perception of the impact that the varying conditions and the simultaneous operation of multiple nodes induce in the overall energy consumption. We present these two sets of experiments in the following section and organise them in two different groups, namely the low-level and the high-level ones.

### 5.1 Low level Experiments

The experimental setup in this first set of experiments consists of just two communicating nodes that operate on the vacant Ch.36 of the 5GHz band. In this setup, we adjust specific PHY-layer configurations and during the protocol operation, we constantly monitor the energy consumption of the individual wireless NICs attached to both the transmitter and receiver nodes. Based on off-line processing of the collected results, we isolate specific events, such as frame transmission or reception and average multiple of them, in order to characterize their instantaneous power consumption, under each specific PHY-layer configuration. In the following experiments, we characterize the power consumption characteristics during frame transmissions under various settings, for both IEEE802.11a/g and IEEE802.11n compatible wireless NICs and present the obtained results in the corresponding sections.

#### 5.1.1 Experimentation with 802.11a/g NICs

In this experiment, we characterize the instantaneous power consumption of the IEEE802.11a/g compatible Atheros AR5424 chipset, during frame transmission events. We start by trans-

mitting frames under fixed PHY-layer Transmission Rate ( $TX_R$ ) values between the 6 Mbps and 54 Mbps that are supported by the IEEE802.11a/g standards. We also fix the Transmission Power ( $TX_P$ ) of the transmitter node at the maximum value of 18 dBm. Based on the collected results, we observe that the power consumed when transmitting frames using different  $TX_R$  does not vary significantly. As frame transmission duration is monotonically related to the configured  $TX_R$ , it is important to quantify energy efficiency in terms of energy consumption per transmitted bit of information ( $E_B$ ). We calculate  $E_B$ , expressed in Joules/bit, as the division of the power consumption values collected for each different  $TX_R$  by the exact  $TX_R$  value expressed in bits/sec. In Fig. 4(a), we plot the obtained  $E_B$  across the available IEEE802.11a/g compatible  $TX_R$  configurations. We notice that higher  $TX_R$  settings always result in lower  $E_B$ , which is mainly due to the decreased duration of frame transmissions.

Next, we fix the  $TX_R$  value and characterize the power consumption of frame transmissions under varying  $TX_P$  settings, by configuring the  $TX_P$  of the transmitter node at the 8 available settings between the values of 18dBm and 0 dBm. Fig. 4(b) presents the instantaneous power consumption across the 8 available  $TX_P$  configurations and under the minimum (6Mbps) and maximum (54 Mbps) available  $TX_R$  settings. We first notice that power consumption decreases monotonically with the decrease of the  $TX_P$  and that the decrease rate varies across different  $TX_R$  configurations. Moreover, we observe that the maximum achievable energy saving of 14% can be obtained in the case that the  $TX_P$  is reduced from the default value of 18 dBm to the minimum one of 0dBm, in the case that  $TX_R$  is set to 6 Mbps.

#### 5.1.2 Experimentation with 802.11n/MIMO NICs

In this second experiment, we investigate the impact of low-level configurations on the energy consumed by the IEEE 802.11n /MIMO compatible Atheros AR9380 chipset, during frame transmission events. The AR9380 chipset is currently the state-of-the-art IEEE802.11n compatible Atheros chipset, featuring 3 RF chains and supporting up to three transmit and receive spatial streams (SS). AR9380 can be configured in 3 different available SS configurations, namely SISO, MIMO2 and MIMO3, where one, two, or three RF-chains are used accordingly. Moreover, each different spatial stream configuration offers 8 different modulation and coding schemes (MCS), resulting in up to 24 different MCS settings for the MIMO3 case. In this experiment, we transmit frames, under fixed MCS indexes among the ones offered in each SS configuration and calculate the instantaneous power consumption in each setting. More specifically, we

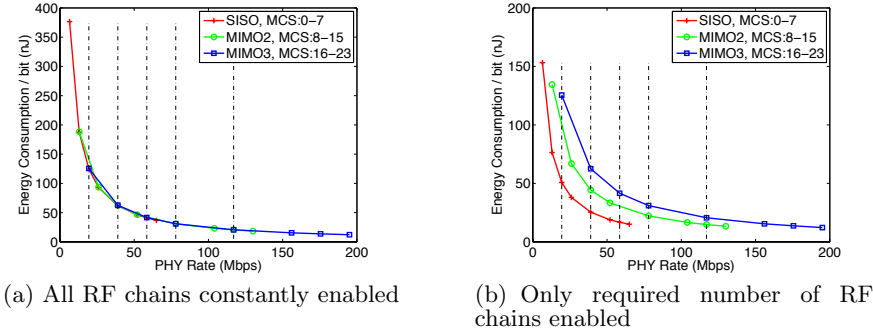


Figure 5: Energy Consumption per bit of AR9380 NIC during transmission across different MCS and Antenna settings

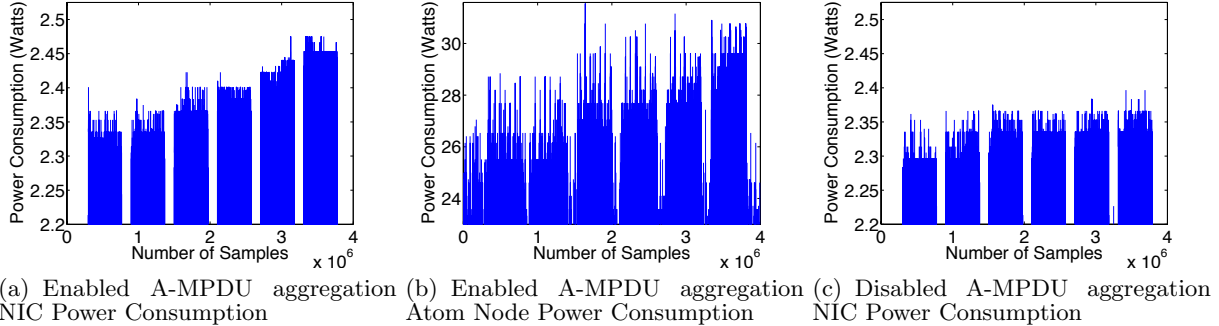


Figure 6: Power Consumption of AR9380 NIC and Atom node during transmission across varying Application-Layer Traffic

use channel bandwidth of 20 MHz and guard interval of 800 ns, resulting in  $TX_R$  settings that range from 6 Mbps in the MCS0 case to 195Mbps in the MCS23 case.

In order to calculate  $E_B$  for the various MCS settings, we follow the procedure described in the previous section. In Fig. 5(a), we plot the obtained  $E_B$  across the 23 available  $TX_R$  configurations, in the case that all RF-chains are constantly enabled, even in cases that the configured SS setting does not use the excess antennas. Based on the collected results, we notice that MCS configurations significantly impact power consumption, as imposed by the calculated  $E_B$ , which ranges from 376.6nJ/bit (MCS0) to 12.2nJ/bit (MCS23). This finding suggests that there exists a huge potential for minimisation of energy expenditure (up to 97%), through proper adaptation of MCS configurations. Fig. 5(b) presents similar results in the case that we enable the exact number of RF-chains that are required by each configured SS setting. In this case, we notice that proper activation of the required number of RF-chains (SISO, MIMO2) can significantly increase energy savings up to 60%, as for the MCS0 case, where  $E_B$  reduces to 153.2nJ/bit. More specifically, we also observe that MCS within the same SS configuration do not remarkably impact power consumption, while MCS indexes of different SS settings result in highly diverse average power consumption values of 0.98W (SISO), 1.75W (MIMO2), 2.45W (MIMO3).

The last part of this experiment has been designed to assess the impact of Application-layer Traffic Rate ( $TR_R$ ) on the consumption of wireless NICs. In this experiment, we fix the MCS index to 23, resulting in the PHY-layer  $TX_R$  value of 195 Mbps. Under this fixed configuration, we run an experiment that varies the  $TR_R$  at the transmitter node in 6 steps, among the values of 10, 20, 50, 100, 200, 300 Mbps. The whole experiment runs for 60 seconds and approximately  $4 \times 10^6$  voltage samples are collected.

Fig. 6(a) illustrates the power consumption of the NIC under the various configured  $TR_R$  values. We clearly observe that increment of Application-layer Traffic Rate results in increased power consumption, where the highest monitored increase of 0.13W, is observed between the 10 and 300Mbps  $TR_R$  values. We also notice that this observation holds even when  $TR_R$  reaches the 300 Mbps value and increases above the capacity limit. However, it is unclear whether the increased energy expenditure is solely related to the increased amount of bytes or also related to the number of frames delivered to the driver. The work in [1], which considered energy consumption on the total node level, revealed and quantified that a substantial proportion of energy is consumed during the packet processing through the Operational System (OS) protocol stack. Moreover, this work suggests that the monitored energy expenditure on the total node level, is primarily associated to the frame processing itself, rather than to the amount of bytes handled. We managed to verify the findings of the work in [1], by measuring the power consumption of an Atom-based node equipped with the AR9380 NIC and by configuring the same  $TR_R$  settings. As illustrated in 6(b), increasing application layer Traffic Rate values result in increased power consumption, where the highest monitored increase of approximately 3.5W, is observed between the 10 and 300Mbps  $TR_R$  values.

Furthermore, in order to assess the impact of PHY-layer A-MPDU frame aggregation on power consumption, we disable frame aggregation and repeat the same experiment. As demonstrated in Fig. 6(c), A-MPDU aggregation slightly increases the resulting power consumption, as monitored for the lowest  $TR_R$  value. However, the monitored trend of increasing power consumption across increasing  $TR_R$  values, is not identified in this case. These observations are rather pioneering and yield interesting insights regarding the impact of traffic load, number of frames delivered to the driver

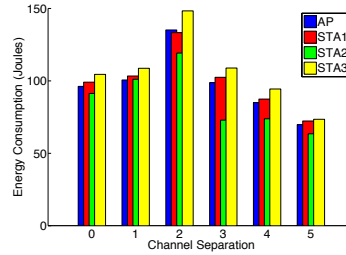
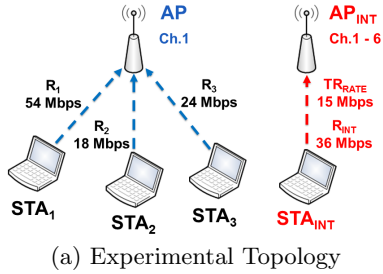


Figure 7: 1st high-level experiment using 802.11a/g compatible NICs

and A-MPDU aggregation on energy consumed by the NIC. However, further investigation is required in order to arrive at safe conclusions, which is not part of this work. Nevertheless, the extended set of presented low-level experiments have clearly demonstrated the advanced energy monitoring capabilities of the NITOS EMF framework.

## 5.2 High level Experiments

The experimental scenario in the following two experiments includes 3 stations (STAs) that are associated with the same access point (AP) and are simultaneously uploading a file of fixed size. The same experiment is repeated under varying channel conditions and different PHY-layer configurations for each wireless NIC, while energy consumption is being constantly monitored. In the first experiment, we use only IEEE802.11a/g compatible NICs, while in the second one IEEE802.11n compatible NICs are employed.

### 5.2.1 1st Experiment based on 802.11a/g NICs

In this experiment, the 3 STAs are simultaneously uploading a file with size of 25MBs, while being associated with the AP that is operating on Ch.1 of the 2.4 GHz band. Another pair of collocated nodes is generating interference, with the station node ( $STA_{INT}$ ) transmitting on uplink at the Application-layer traffic load of 15Mbps. Fig. 7(a) illustrates the experimental topology along with the PHY-layer rate settings of each specific NIC. The experiment is repeated 6 times, where in each different run we configure the  $AP_{INT}$  to operate on a different channel between Ch.1 and Ch.6 of the 2.4 GHz band.

During each different run, we monitor the energy consumption of each NIC and plot the collected results in Fig. 7(b). While  $AP_{INT}$  moves from Ch.1 to Ch.2 and subsequently to Ch.3, we notice that the total energy consumption of all NICs is increased. Due to adjacent channel interference, transmissions of  $STA_{INT}$  are not always detected by the three STAs, which results in frame collisions and subsequent frame retransmissions. The overall effect is that the file transmission durations are increased for each individual node and thus impact the overall energy expenditure. As  $AP_{INT}$  moves from Ch.3 to Ch.5, we notice that the energy consumption tends to decrease for all NICs, resulting in the lowest monitored values in the case that the interfering link operates on Ch.6, as it no more interferes with the 3 STAs.

A particular observation in all cases is related to the energy performance of STA2. While STA2 uses the lowest PHY-layer rate of 18 Mbps, compared to the rates of STA1 (54Mbps) and STA3 (24Mbps), it manages to result in the lowest energy expenditure in all cases. This comes in contrast with the higher  $E_B$  values that the lower PHY-layer

rates correspond to. However, this uniquely identified performance results due to the fact that STA2 completes the file uploading sooner than the rest nodes, in all cases. Based on the experimental log files, we observe that STA2 always achieves the highest throughput. The increased throughput performance of STA2 can only be associated with the "Capture Effect" phenomenon [28], due to which certain topology configurations result in unfair throughput distribution for specific links.

### 5.2.2 2nd Experiment based on 802.11n/MIMO NICs

In this second experiment, the 3 STAs follow the same file uploading process, while the AP is operating on Ch. 36 of the 5 GHz band, using a channel bandwidth of 40MHz. However, in this scenario MIMO enabled NICs are used and the size of the file to be uploaded is 1 GB. We statically fix the single (SS) stream configuration for STA1, while STA2 and STA3 are configured with the double (DS) and triple (TS) stream setting accordingly. We also enable the default MCS adaptation mechanism of the driver, which results in the assignments of MCS7 for STA1, MCS15 for STA2 and MCS21 for STA3, as presented in Fig. 8(a). The experiment is executed in two phases, where in the first phase each node completes the file uploading, using the medium in an *individual* way, as the rest two STAs are disabled. In the second phase, we configure the 3 STAs to transmit simultaneously and monitor energy performance, during the execution of the *combined* experiment.

Fig. 8(b) depicts the total energy consumed by each individual wireless NIC, as monitored during both phases of the experiment. In the first phase, we notice that the AP results in the lowest energy expenditure, which comes from the fact that it operates in reception mode, in which case the energy consumption is significantly less compared with the consumption during transmission. We also notice that STA3 using the TS mode consumes the highest amount of energy (8.53J), while STA1(7.04J) and STA2 (6.25J) follow accordingly. In this case, the energy performance of all nodes is directly related with the  $E_B$  that each different MCS index is characterized by, which values are 7.705nJ/bit, 7.535nJ/bit and 6.66nJ/bit for MCS21, MCS7 and MCS15 accordingly.

In the second phase, we observe that average energy consumption is significantly increased for all nodes, resulting due to the decrease in channel access opportunities and the corresponding increase of idle listening periods. More specifically, STA3 again consumes the highest amount of energy (24.61J), while STA2(16.75J) and STA1(9.22J) follow accordingly. In this case, energy performance cannot be associated with the  $E_B$  parameter, as it does not consider the amount of time spent during idle listening periods. Based

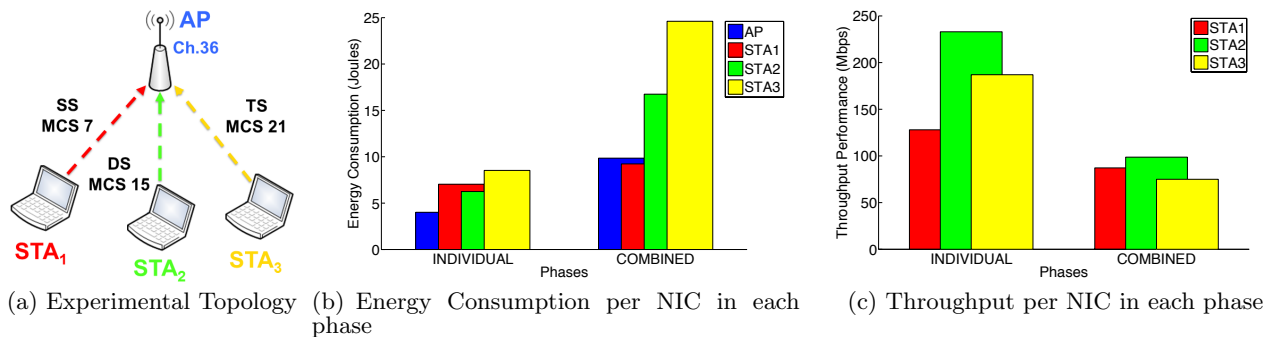


Figure 8: 2nd high-level experiment using 802.11n compatible NICs

on the throughput performance evaluation, which is illustrated in Fig. 8(c), we notice that in the combined experiment all nodes achieve nearly equal performance, which results in approximately equal time spent for the completion of the file uploading process. In this case, NICs that enable higher number of RF-chains and result in higher instantaneous power consumption, eventually induce higher total energy consumption within the same experiment duration.

As clearly demonstrated through the two high level experiments, important factors, such as topology and interference conditions and interaction among simultaneously transmitting nodes, can greatly impact energy expenditure. Due to the inherent inability of power consumption models to accurately analyze energy consumption in such complex scenarios, online energy consumption monitoring needs to be applied, in order to arrive at concrete conclusions.

## 6. CONCLUSIONS AND FUTURE WORK

In this work, we introduced the novel NITOS EMF framework that is able to characterise the consumption of wireless testbed infrastructure in an online way. The proposed framework is built on a distributed network of low-cost, but highly accurate devices and is fully integrated with the large-scale wireless NITOS testbed. Through extensive experiments, we demonstrated the advanced platform capabilities that can aid towards energy performance assessment of realistic testbed experiments. As part of our future work, we plan on connecting the framework with the available software defined radio and sensor hardware of NITOS and extend the range of collected measurements.

## 7. ACKNOWLEDGEMENTS

The authors acknowledge the support of the European Commission through IP project OpenLab (FP7-287581) and STREP project Stamina (FP7-265496). Moreover, the authors would like to thank Akis Chanos for his valuable help during the initial hardware modifications and testing.

## 8. REFERENCES

- [1] A. Garcia-Saavedra, P. Serrano, A. Banchs, and G. Bianchi. Energy consumption anatomy of 802.11 devices and its implication on modeling and design. In *Proceedings of CoNEXT*, 2012.
- [2] N. Balasubramanian, A. Balasubramanian, and A. Venkataramani. Energy consumption in mobile phones: A measurement study and implications for network applications. In *Proceedings of IMC*, 2009.
- [3] J. Tarascon. Key challenges in future Li-battery research. *Philos Trans A Math Phys Eng Sci*, pages 3227–4, 2010.
- [4] X. Zhang and K. Shin. EMiLi: energy-minimizing idle listening in wireless networks. In *Proceedings of Mobicom*, 2011.
- [5] Kishore R., Ravi K., Honghai Z., and Marco G. Symphony: Synchronous Two-phase Rate and Power Control in 802.11 WLANs. In *Proceedings of Mobisys*, 2008.
- [6] J. Manweiler and R. R. Choudhury. Avoiding the rush hours: WiFi energy management via traffic isolation. In *Proceedings of MobiSys*, 2011.
- [7] M. Ra, J. Paek, A. B. Sharma, R. Govindan, M. H. Krieger, and M. J. Neely. Energy-delay tradeoffs in smartphone applications. In *Proceedings of MobiSys*, 2010.
- [8] "Tmote sky Specifications", <http://goo.gl/Tc9qR>.
- [9] "MICAz Specifications", <http://goo.gl/rLYHU>.
- [10] "Atheros White Paper - Power Consumption and Energy Efficiency Comparisons".
- [11] "NITOS Wireless Testbed", <http://nitlab.inf.uth.gr>.
- [12] K. Jang, S. Hao, A. Sheth, and R. Govindan. Snooze: energy management in 802.11n WLANs. In *Proceedings of CoNEXT*, 2011.
- [13] C. Li, C. Peng, S. Lu, and X. Wang. Energy-based rate adaptation for 802.11n. In *Proceedings of Mobicom*, 2012.
- [14] D. Halperin, B. Greenstein, A. Sheth, and D. Wetherall. Demystifying 802.11n power consumption. In *Proceedings of SIGOPS HotPower*, 2010.
- [15] A. Hergenroder, J. Horneber, and J. Wilke. SANDbed: A WSN Testbed for Network Management and Energy Monitoring. In *GIITG KuVS Sensornetze*, 2009.
- [16] A. Kipp, J. Liu, T. Jiang, J. Bucholz, L. Schubert, M. Berge, and W. Christmann. Testbed architecture for generic, energy-aware evaluations and optimisations. In *Infocomp*, 2011.
- [17] K. Gomez, R. Riggio, T. Rashed, D. Miorandi, and F. Granelli. Energino: Hardware and Software Solution for Energy Consumption Monitoring. In *Proceedings of WiOpt*, 2012.
- [18] G. Kazdaridis, S. Keranidis, H. Niavis, T. Korakis, I. Koutsopoulos, and L. Tassioulas. An Integrated Chassis Manager Card Platform Featuring Multiple Sensor Modules. In *Proceedings of Tridentcom*, 2012.
- [19] "Arduino Mega 2560 Board", <http://goo.gl/IFHwq>.
- [20] "Texas Instruments INA139", <http://goo.gl/rPQLB>.
- [21] "Advanced Arduino ADC", <http://goo.gl/AwQ95>.
- [22] "Enhancing Arduino's ADC", <http://goo.gl/BRXCX>.
- [23] "Atmega ADC accuracy vs clock speed", <http://goo.gl/qTlhx>.
- [24] "NI-6210 DAQ module", <http://goo.gl/oFSJw>.
- [25] "OMF-control & Management Framework", <http://omf.mytestbed.net/>.
- [26] "OML Measurement Library", <http://mytestbed.net/projects/oml/wiki/>.
- [27] "Energy Characteristics of NITOS NICs", <http://nitlab.inf.uth.gr/NITlab/papers/EnergyTR.pdf>.
- [28] J. Lee, W. Kim, S. Lee, D. Jo, J. Ryu, T. Kwon, and Y. Choi. An experimental study on the capture effect in 802.11a networks. In *ACM WinTECH*, 2007.